

Three -Pion Correlations

Minoru Biyajima*

Department of Physics, Shinshu University, Matsumoto 390-8621, Japan

E-mail: biyajima@azusa.shinshu-u.ac.jp

Takuya Mizoguchi

Toba National College of Maritime Technology, Toba 517-8501, Japan

E-mail: mizoguti@toba-cmt.ac.jp

Naomichi Suzuki

Department of Comprehensive Management, Matsumoto University, Matsumoto 390-1295, Japan

E-mail: suzuki@matsu.ac.jp

First of all, we mention the situation of empirical analyses on 3rd order BEC (Bose-Einstein Correlation) at RHIC. Second, we introduce several theoretical formulae / approaches. Third we present our analyses of data in Au+Au at 130 GeV by STAR and preliminary data in Au+Au at 200 GeV by PHENIX Collaborations. Our results also contain analyses by means of core-halo model. Finally, we estimate that the volume of interaction in Au + Au collisions at 130 GeV is 500 fm^3 , which is compared with $V = R_{\text{long}}R_{\text{out}}R_{\text{side}} \sim 300 \text{ fm}^3$ in Pb + Pb collision at 2.76 TeV by ALICE Collaboration. Moreover, usefulness of empirical analyses on $(2\pi^+)\pi^-$ and $(2\pi^-)\pi^+$ combinations at RHIC and LHC energies is remarked.

The Seventh Workshop on Particle Correlations and Femtoscopy

September 20 - 24 2011

University of Tokyo, Japan

*Speaker.

1. Situation of Empirical analyses on 3rd order BEC in Au+Au collision at RHIC

As shown in Table 1, STAR and PHENIX Coll. have reported their analyses at 130 GeV and 200 GeV, respectively. In their analyses, STAR Coll. [1] used all combinations of three momentum-transfers $\sqrt{q_{ij}^2} \leq Q_3$ (Inside of a globe in Fig. 1),

$$Q_{inv,3}^2 = q_{12}^2 + q_{23}^2 + q_{31}^2. \quad (1.1)$$

On the other hand, PHENIX Coll. [2] used data on diagonal line of a cube in Fig. 1,

$$q_3 = \langle q_{12} \rangle = \langle q_{23} \rangle = \langle q_{31} \rangle \quad \text{i.e.} \quad Q_{inv,3}^2 = 3q_3^2. \quad (1.2)$$

Of course this relation holds, as the number of data increases. $\langle \dots \rangle$ is an average value.

Table 1: Situation of analyses on the 3rd order BEC. Notice two empty columns.

$\sqrt{s_{NN}}$	STAR	PHENIX
130 GeV	raw and corrected data by Q_{inv}	
200 GeV		preliminary raw and corrected data by q_3

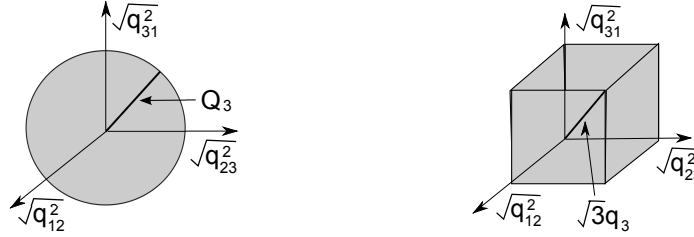


Figure 1: Data ensembles of STAR (left) and PHENIX Coll (right).

Here we compare two kinds of data. In Figs. 2, data by PHENIX Coll. are rearranged by $\sqrt{3}q_3$. Coincidence among data by STAR and PHENIX Coll is fairly good. Error bars in raw data by PHENIX Coll are smaller than those of STAR Coll.

2. Several theoretical formulae

In many analyses on BEC, the following formulae based on plane wave function are used.

$$N^{(2\pi)}/N^{BG} = c \left[1 + \lambda e^{-(RQ)^2} \right], \quad (2.1)$$

$$N^{(3\pi)}/N^{BG} = c \left[1 + \lambda \sum_{i>j} e^{-(RQ_{ij})^2} + 2\lambda^{1.5} e^{-0.5(RQ_3)^2} \right]. \quad (2.2)$$

In laser optical (LO/GL) approach, the following formulae with a degree of chaoticity p have been proposed [3] and utilized,

$$N^{(2\pi)}/N^{BG} = 1 + 2p(1-p)E_{2B} + p^2 E_{2B}^2, \quad (2.3)$$

$$N^{(3\pi)}/N^{BG} = 1 + 6p(1-p)E_{3B} + 3p^2(3-2p)E_{3B}^2 + 2p^3 E_{3B}^3, \quad (2.4)$$

where $E_{2B}^2 = \exp(-R^2 Q^2)$ (Gaussian form) and/or $E_{2B}^2 = \exp(-R\sqrt{Q^2})$ (exponential form), and $E_{3B}^3 = \exp(-R^2 Q_3^2)$ and so on.

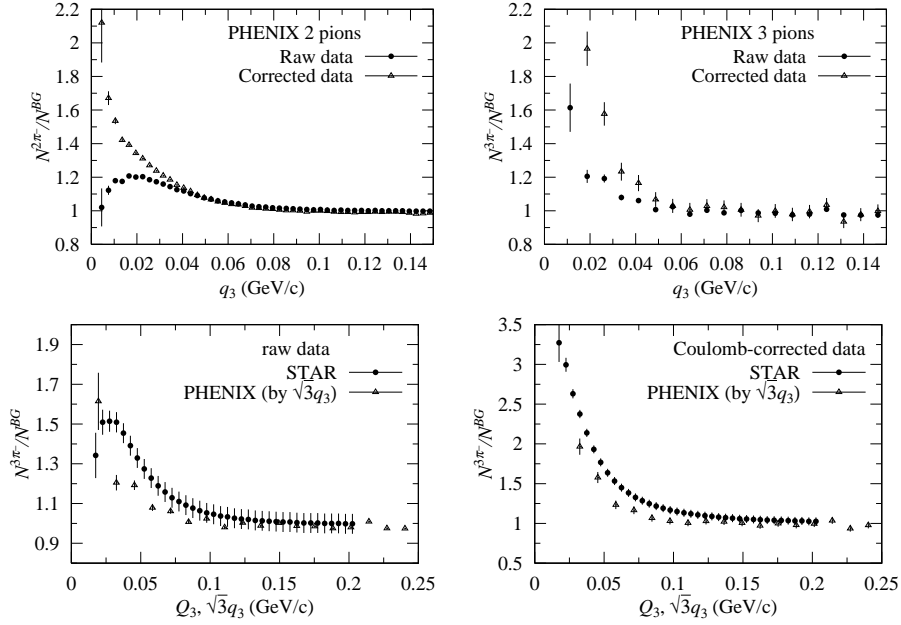


Figure 2: Comparisons of data by STAR and PHENIX Coll.

Third we explain the formulae by Coulomb wave function including the degree of coherence λ and the interaction range R [4, 5, 6, 7]. The two-body Coulomb wave function is well known as,

$$\psi_{k_{ij}}^C(x_i x_j) = \Gamma(1 + i\eta_{ij}) e^{\pi\eta_{ij}/2} e^{ik_{ij} \cdot r_{ij}} F[-i\eta_{ij}, 1; i(k_{ij}r_{ij} - k_{ij} \cdot r_{ij})], \quad (2.5)$$

where, $r_{ij} = x_i - x_j$, $k_{ij} = (k_i - k_j)/2$, $r_{ij} = |r_{ij}|$, $k_{ij} = |k_{ij}|$ and $\eta_{ij} = e_i e_j \mu_{ij} / k_{ij}$. μ_{ij} : reduced mass of m_i and m_j , $F[a, b; x]$: confluent hypergeometric function, $\Gamma(x)$: Gamma function.

Using of Eq. (2.5), the 2nd order BEC with λ and Gaussian form for $\rho(x_i)$ is calculated as,

$$\begin{aligned} N^{(2\pi^-)} &= \frac{1}{2} \prod_{i=1}^2 \int \rho(x_i) d^3 x_i |\psi_{k_1 k_2}^C(x_1, x_2) + \psi_{k_1 k_2}^C(x_2, x_1)|^2 \\ &= \prod_{i=1}^2 \int \rho(x_i) d^3 x_i \left[\frac{1}{2} (|\psi_{k_1 k_2}^C(x_1, x_2)|^2 + |\psi_{k_1 k_2}^C(x_2, x_1)|^2) \right. \\ &\quad \left. + \lambda \text{Re} \left(\psi_{k_1 k_2}^C(x_1, x_2) \psi_{k_1 k_2}^{C*}(x_2, x_1) \right) \right], \end{aligned} \quad (2.6)$$

The 3rd order BEC is computed based on the 3-body Coulomb wave function in [6],

$$\Psi_f = \psi_{k_1 k_2}^{C'}(x_1, x_2) \psi_{k_2 k_3}^{C'}(x_2, x_3) \psi_{k_3 k_1}^{C'}(x_3, x_1), \quad (2.7)$$

Hereafter, we use the following expression; $\psi_{k_i k_j}^{C'}(x_i, x_j) = e^{i(2/3)k_{ij}r_{ij}} \phi_{k_{ij}}(r_{ij})$. Notice that the numerical factor “2/3” in the exponential function is important [6, 7].

$$N^{(3\pi^-)} = \frac{1}{6} \prod_{i=1}^3 \int \rho(x_i) d^3 x_i \left| \sum_{j=1}^6 A(j) \right|^2, \quad (2.8)$$

where

$$\begin{aligned} A(1) &= A_1 = \psi_{k_1 k_2}^{C'}(x_1, x_2) \psi_{k_2 k_3}^{C'}(x_2, x_3) \psi_{k_3 k_1}^{C'}(x_3, x_1), \\ A(2) &= A_{23} = \psi_{k_1 k_2}^{C'}(x_1, x_3) \psi_{k_2 k_3}^{C'}(x_3, x_2) \psi_{k_3 k_1}^{C'}(x_2, x_1). \end{aligned} \quad (2.9)$$

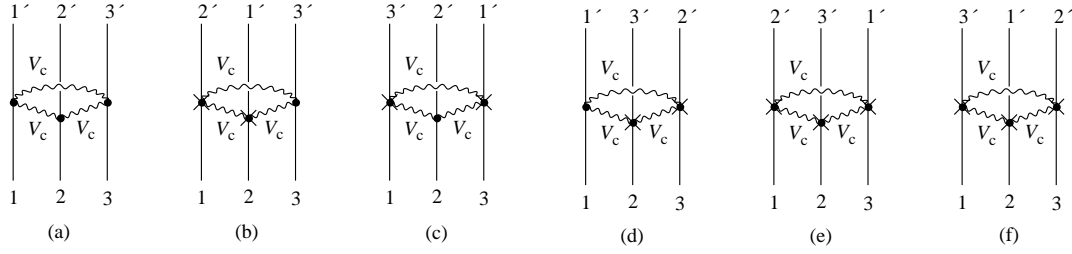


Figure 3: Diagrams of the 3rd order BEC for $A(1) \sim A(6)$.

A_{ijk} is reflecting the permutations of particles, i, j, k in Fig. 3: Therein $A(3) = A_{12}$, $A(4) = A_{123}$, $A(5) = A_{132}$ and $A(6) = A_{13}$. In the plane wave approx., we have the correct expression, where $A(3) \sim A(6)$ are skipped [5, 7],

$$\begin{aligned} A(1) &= A_1 \xrightarrow{\text{PW}} e^{i(2/3)(k_{12} \cdot r_{12} + k_{23} \cdot r_{23} + k_{31} \cdot r_{31})} = e^{i(k_1 \cdot x_1 + k_2 \cdot x_2 + k_3 \cdot x_3)}, \\ A(2) &= A_{23} \xrightarrow{\text{PW}} e^{i(2/3)(k_{12} \cdot r_{13} + k_{23} \cdot r_{32} + k_{31} \cdot r_{21})} = e^{i(k_1 \cdot x_1 + k_2 \cdot x_3 + k_3 \cdot x_2)}. \end{aligned} \quad (2.10)$$

Combining $A(1) \sim A(6)$ in Fig. 3, we obtain F_1 as: (The other formulae $F_{12} \sim F_{123}$ and F_{132} are given in [6, 7].)

$$F_1 = \frac{1}{6} [A_1 A_1^* + A_{12} A_{12}^* + A_{23} A_{23}^* + A_{13} A_{13}^* + A_{123} A_{123}^* + A_{132} A_{132}^*]. \quad (2.11)$$

$$\begin{aligned} \frac{N^{3\pi^-}}{N^{BG}} &= C \prod_{i=1}^3 \int \rho(x_i) d^3 x_i \left[F_1 + 3\lambda F_{12} + 2\lambda^{\frac{3}{2}} \text{Re}(F_{123}) \right] \\ &= \frac{C}{(2\sqrt{3}\pi R^2)^3} \int d^3 \zeta_1 d^3 \zeta_2 \exp \left[-\frac{1}{2R^2} \left(\frac{1}{2} \zeta_1^2 + \frac{2}{3} \zeta_2^2 \right) \right] \left[F_1 + 3\lambda F_{12} + 2\lambda^{\frac{3}{2}} \text{Re}(F_{123}) \right] \end{aligned} \quad (2.12)$$

where $\zeta_1 = x_2 - x_1$, $\zeta_2 = x_3 - (m_1 x_1 + m_2 x_2)/M_2$, $\zeta_3 = (m_1 x_1 + m_2 x_2 + m_3 x_3)/M$, $M_2 = m_1 + m_2$ and $M = m_1 + m_2 + m_3$.

Finally, it is known that the core-halo model is a useful model. However, explicit expressions are skipped here. See our studies in [4, 5, 6, 7]. See also [8].

3. Analyses of data by STAR Coll and PHENIX Coll

3-1) For Coulomb corrected data, we employ the conventional formulae, Eqs. (2.1) and (2.2). Ours are given in Table 2 and Fig. 4. It is interesting that $R_{2\pi} \sim R_{3\pi} \sim 8.5$ fm for data by STAR Coll.

Table 2: Analyses of corrected data by STAR and PHENIX Coll (Eqs. (2.1) and (2.2).)

	STAR			PHENIX		
	R [fm]	λ	$\chi^2/\text{n.d.f.}$	R [fm]	λ	χ^2/N_{dof}
$2\pi^-$	8.75 ± 0.31	0.58 ± 0.02	23.0/25	4.77 ± 0.04	0.39 ± 0.01	178/40
$3\pi^-$	8.26 ± 0.39	0.50 ± 0.02	1.88/35	6.92 ± 0.82	0.34 ± 0.10	6.5/14

3-2) Corrected data with $q_3 > 0.02$ GeV by PHENIX Coll are analyzed by conventional formula / LO approach. Our results are shown in Figs. 4 and 5, and Tables 2 and 3.

3-3) Raw data with $q_3 > 0.02$ GeV are analyzed by the formulae of Coulomb wave function (Eqs. (2.6) and (2.12)). Our results are also shown in Fig. 6 and lower-part of Table 3.

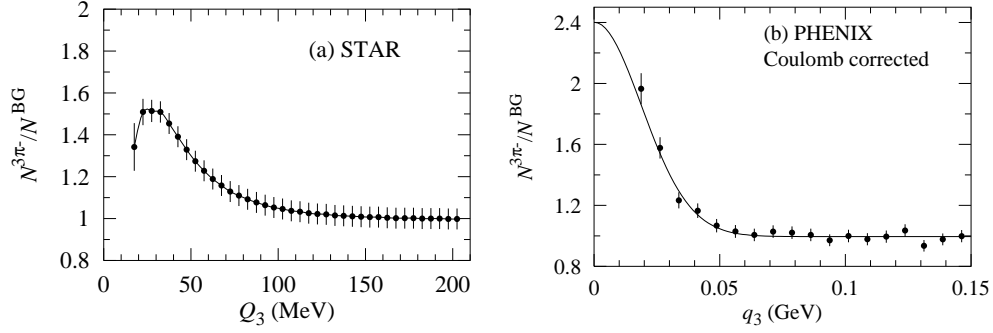


Figure 4: Analyses of corrected data by STAR Coll. and PHENIX Coll. Eqs. (2.1) and (2.2) are used.

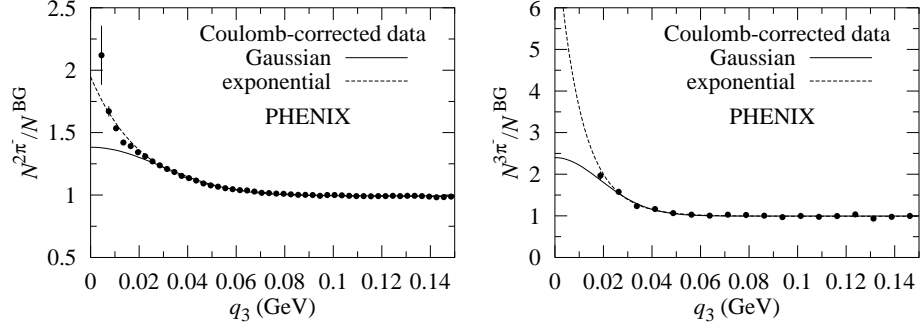


Figure 5: Corrected data are analyzed by Eq. (2.3) and (2.4)

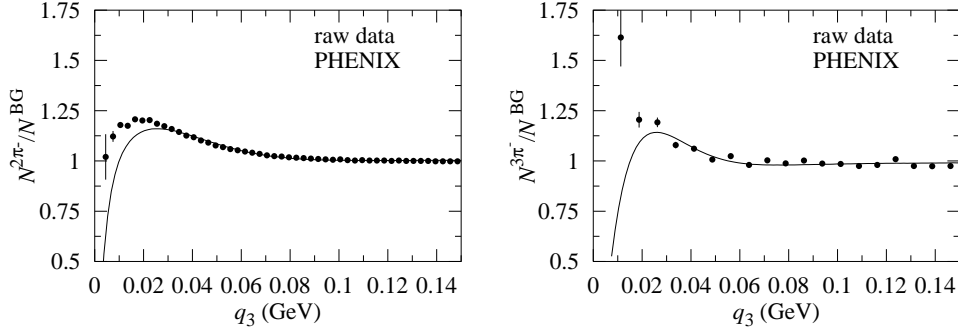


Figure 6: Analyses of raw data by PHENIX Coll. Eqs. (2.6) and (2.12) are used.

3-4) Using two formulae in the core-halo approach (with Gaussian source function, the fraction of core part f_c and the degree of coherent p_c in [5, 6, 7]) we obtain Fig. 7. In raw data, there is no over-lapping region. On the other hand, in corrected data, we observe very narrow over-lapping region. The reason of the wide region of 3π BEC is due to large error bars of corrected data [2].

4. Summary

4-1) From raw data as well as Coulomb corrected data in Au+Au at 130 GeV by STAR Coll., we get the following interaction ranges $R_{2\pi} = 8.7$ fm and $R_{3\pi} = 8.3$ fm, and can estimate

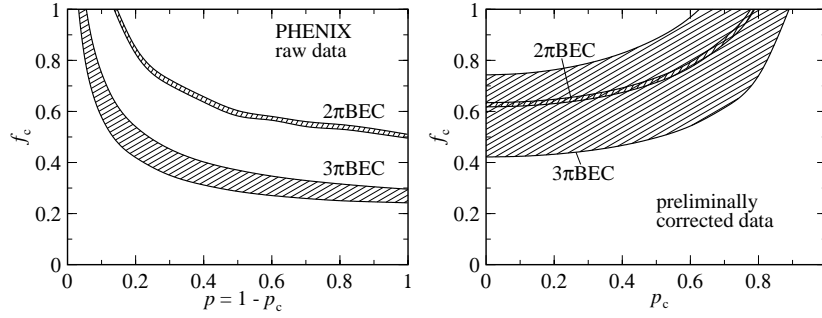
$$V = R_{3\pi}^3 \sim 500 \text{ fm}^3. \quad (4.1)$$

This value is compared with that of ALICE Coll [9], $V = R_{\text{long}} R_{\text{out}} R_{\text{side}} \sim 300 \text{ fm}^3$ at $dN_{ch}/d\eta = 1500$ and $k_T \sim 0.3$ GeV in Pb+Pb at 2.76 TeV.

4-2) On the contrary, from corrected data at 200 GeV by PHENIX Coll., we obtain the ranges, by utilizing Eqs. (2.1) and (2.2), $R_{2\pi} = 4.8$ fm ($\lambda = 0.39$) and $R_{3\pi} = 6.9$ fm ($\lambda = 0.34$). From raw

Table 3: Analyses of data by PHENIX Coll. Eqs. (2.3), (2.4), (2.6) and (2.12) are used.

E_{2B}		R [fm]	p	c	χ^2/N_{dof}
2π	Gaussian	6.58 ± 0.05	0.23 ± 0.00	0.98 ± 0.00	156/40
	Exponential	9.54 ± 0.16	0.99 ± 0.01	0.99 ± 0.00	56/40
3π	Gaussian	9.76 ± 1.11	0.24 ± 0.08	0.99 ± 0.00	7.2/14
	Exponential	14.36 ± 2.10	1.00 ± 0.07	0.99 ± 0.02	6.3/14
raw data		R (fm)	λ	c	χ^2/N_{dof}
2π	Eq. (2.6)	3.77 ± 0.03	0.253 ± 0.004	1.00 ± 0.00	129/40
3π	Eq. (2.12)	5.77 ± 0.32	0.19 ± 0.02	1.00 ± 0.00	84/14

**Figure 7:** Analyses of data by core-halo model.

data, we have smaller interaction ranges $R_{2\pi} = 3.8$ fm and $R_{3\pi} = 5.8$ fm. The interaction ranges of data at 200 GeV by PHENIX Coll. are smaller than those of STAR Coll. At present, it is difficult to draw concrete physical picture for Au+Au collision at 200 GeV. Then we are waiting for final empirical analyses by PHENIX Coll.

4-3) Moreover, we also eager for empirical analyses of $(2\pi^+)\pi^-$ and $(2\pi^-)\pi^+$ combinations at RHIC and LHC energies. See [10, 11].

References

- [1] J. Adams *et al.* [STAR Collaboration], Phys. Rev. Lett. **91**, 262301 (2003).
- [2] M. Csanad [PHENIX Collaboration], Nucl. Phys. A **774**, 611 (2006).
- [3] M. Biyajima, A. Bartl, T. Mizoguchi, O. Terazawa and N. Suzuki, Prog. Theor. Phys. **84**, 931 (1990) [Addendum-ibid. **88**, 157 (1992)].
- [4] T. Mizoguchi and M. Biyajima, Phys. Lett. B **499**, 245 (2001)
- [5] M. Biyajima, M. Kaneyama and T. Mizoguchi, Phys. Lett. B **601**, 41 (2004).
- [6] M. Biyajima, T. Mizoguchi and N. Suzuki, Phys. Lett. B **637**, 64 (2006).
- [7] M. Biyajima, T. Mizoguchi and N. Suzuki, AIP Conf. Proc. **828**, 589 (2006).
- [8] T. Csorgo, B. Lorstad, J. Schmid-Sorensen and A. Ster, Eur. Phys. J. C **9**, 275 (1999).
- [9] K. Aamodt *et al.* [ALICE Collaboration], Phys. Lett. B **696**, 328 (2011).
- [10] M. Biyajima, T. Mizoguchi and N. Suzuki, Phys. Lett. B **568**, 237 (2003).
- [11] P. Abreu *et al.* [DELPHI Collaboration], Phys. Lett. B **355**, 415 (1995).